[Article] Numerical study of the noninertial systems: applicationto train coupler systems

Numerical study of the noninertial systems: application to train coupler systems

Alberto Massa · Luca Stronati · Ahmed K. Aboubakr · Ahmed A. Shabana · Nicola Bosso

Abstract Car coupler forces have a significant effect on the longitudinal train dynamics and stability. Because the coupler inertia is relatively small in comparison with the car inertia; the high stiffness associated with the coupler components can lead to high frequencies that adversely impact the computational efficiency of train models. The objective of this investigation is to study the effect of the coupler inertia on the train dynamics and on the computational efficiency as measured by the simulation time. To this end, two different models are developed for the car couplers; one model, called the *inertial coupler model*, includes the effect of the coupler inertia, while in the other model, called the *noninertial model*, the effect of the coupler inertia is neglected. Both inertial and noninertial coupler models used in this investigation are assumed to have the same coupler kinematic degrees of freedom that capture geometric nonlinearities and allow for the relative translation of the draft gears and end of car cushioning (EOC) devices as well as the relative rotation of the coupler shank. In both models, the coupler kinematic equations are expressed in terms of the car body and coupler coordinates. Both the inertial and noninertial models used in this study lead to a system of differential and algebraic equations that are solved simultaneously in order to determine the coordinates of the cars and couplers. In the case of the inertial model, the coupler kinematics is described using the absolute Cartesian coordinates, and the algebraic equations describe the kinematic constraints imposed on the motion of the system. In this case of the inertial model, the constraint equations are satisfied at the position, velocity, and acceleration levels. In the case of the noninertial model, the equations of motion are developed using the relative joint coordinates, thereby eliminating systematically the algebraic equations that represent the kinematic constraints. A quasistatic force analysis is used to determine a set of coupler nonlinear force algebraic equations for a given car configuration. These nonlinear force algebraic equations are solved iteratively to determine the coupler *noninertial coordinates* which enter into the formulation of the equations of motion of the train cars. The results obtained in this study showed that the neglect of the coupler inertia eliminates high frequency oscillations that can negatively impact the computational efficiency. The effect of these high frequencies that are attributed to the coupler inertia on the simulation time is examined using frequency and eigenvalue analyses. While the neglect of the coupler inertia leads, as demonstrated in this investigation, to a much more efficient model, the results obtained using the inertial and noninertial coupler models show good agreement, demonstrating that

A. Massa · L. Stronati · N. Bosso
Dipartimento di Meccanica, Politecnico di Torino, C. so Duca Degli Abruzzi 24, 10129, Torino, Italy

A.K. Aboubakr · A.A. Shabana (✉)
Department of Mechanical and Industrial Engineering, University of Illinois at Chicago, 842 West Taylor Street, Chicago, IL 60607, USA
e-mail: shabana@uic.edu

the coupler inertia can be neglected without having an adverse effect on the accuracy of the solution.

Keywords Longitudinal train forces · Coupler geometric nonlinearities · Railroad vehicle dynamics · Multibody systems

1 Introduction

Accurate prediction of coupler forces is necessary in the analysis of train longitudinal dynamics and stability. In order to achieve higher degree of computational efficiency, longitudinal train dynamics (LTD) algorithms tend to be simpler as compared to the more general multibody system (MBS) algorithms which require the solution of a system of differential/algebraic equations (DAE's). The algebraic equations that relate redundant coordinates in MBS algorithms must be satisfied at the position, velocity, and acceleration levels. The use of redundant coordinates in MBS algorithms leads to a sparse matrix structure that can be exploited in order to efficiently solve the dynamic equations of motion. Most LTD algorithms, on the other hand, do not employ a DAE's solver, and they use independent coordinates instead of redundant coordinates. The equations of motion are expressed in terms of the system degrees of freedom by systematically eliminating dependent variables. Nonetheless, the implementation of efficient force elements may necessitate introducing algebraic equations in LTD algorithms as will be discussed in this investigation.

Train car couplers, which are designed to absorb shock forces resulting from sudden brake applications and traction, include elastic, viscoelastic, and/or friction elements. While in many investigations on train longitudinal dynamics, the couplers are represented by massless discrete spring-damper elements, MBS algorithms allow for the development of detailed models that capture the coupler geometric nonlinearities resulting from the relative rotations of the coupler components. In order to develop such detailed MBS coupler and train models, most MBS algorithms take into account the effect of the coupler inertia. However, because couplers have high stiffness and small inertia in comparison with the train car inertia, including the effect of the coupler inertia in the dynamic model can lead to high frequency oscillations that can adversely affect the computational efficiency. One example of a coupler that has such a high stiffness coupling element is the knuckle-type automatic coupler, which connects firmly when one car is bumped against another. This coupler was introduced in the 1880s and is still in use despite the fact that improved designs are available [5]. The use of the automatic coupler in North America became standard in 1917 with the introduction of the knuckle coupler, also called buckeye coupler or Janney coupler [8] that replaced the Miller Hook which was never widely used in freight vehicles to replace the link and pin coupling system [5]. The knuckle coupler, shown schematically in Fig. 1, consists of a knuckle attached to the end of a shank fastened to a housing mechanism on the car. The assembly is designed to allow for some lateral play in order to avoid derailments during curve negotiations. Cars are automatically coupled by engaging the open knuckle on one car to a closed knuckle on the other car. A conventional auto-coupler package is shown in Fig. 2 [4]. The coupler element consists of a head and shank that can be connected to a flexible unit such as a draft gear or an end-of-car-cushioning (EOC) device that is attached to the car body. The draft gear and EOC device are energy dissipating elements; the draft gear employs dry friction using friction wedges, while the EOC device includes oil-based dashpots (dampers) that produce damping force that depends on the rela-tive velocity [4, 6]. It is known that longitudinal train forces during braking, traction, and curve negotiations heavily depend on the design of the couplers, their de-grees of freedom, and their ability to absorb impact forces and dissipate energy. For this reason, differ-ent coupler designs, with the improvements made over many years, are studied extensively in order to exam-ine their performance and their effect on railroad vehi-cle system dynamics and stability [10, 17].

2 Scope and objective of this investigation

As previously mentioned, in most railroad vehicle computer formulations, the coupler is modeled as a spring-damper element with no kinematic degrees of freedom [11]. The force in this spring-damper element is function of the relative displacements between the two cars connected by this coupler. This simplified ap-proach does not take into account the effect of the cou-pler degrees of freedom and fails to capture the cou-pler geometric nonlinearities that can influence the car

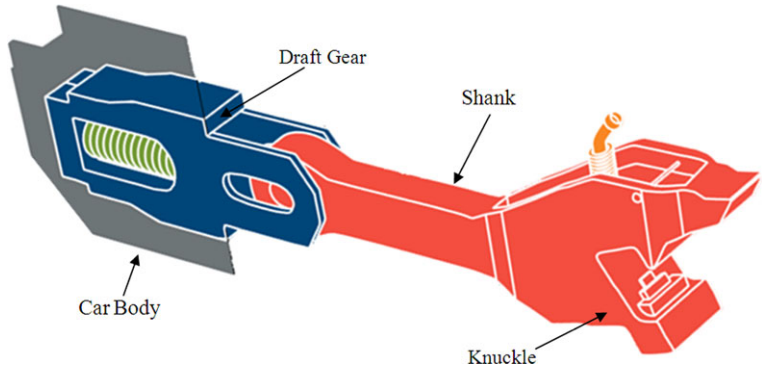

Fig. 1 Automatic coupler

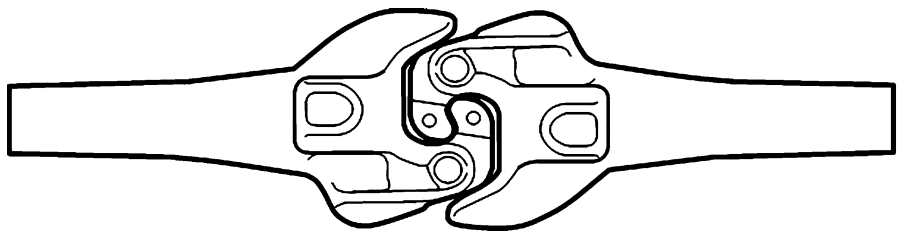

Fig. 2 Conventional auto-coupling package

motion. Developing a more accurate coupler model requires including coupler kinematic degrees of freedom that account for the geometric nonlinearities resulting from the motion of the coupler components. For such a detailed coupler model, two fundamentally different approaches that require the use of two different solution procedures can be used. In the first approach, the inertia of the coupler is taken into account. In such a model, called *inertial coupler model*, the algebraic equations, if they are present in the model, describe connectivity constraint equations which must be satisfied at the position, velocity, and acceleration levels since the coupler accelerations appear in the equations of motion. The coupler degrees of freedom have generalized inertia forces associated with them and, therefore, their second derivatives appear in the system equations of motion. This leads to an increase in the number of the system state equations that must be integrated numerically.

In the second approach, on the other hand, the inertia of the coupler, assumed small compared to the car body inertia, is neglected. In this model, called the *noninertial coupler model*, no generalized inertia forces are associated with the coupler degrees of freedom, and as a consequence, the second derivatives of these coordinates do not appear in the final form of the equations of motion. The use of such noninertial coupler model can lead to significant reduction in the number of state equations and can also contribute to eliminating the high frequency oscillations that might result from the high coupler stiffness and its relatively small inertia. A set of quasistatic coupler equilibrium conditions can be developed and used to define a set of nonlinear algebraic equations that can be solved iter-atively for the coupler noninertial coordinates. These coupler noninertial coordinates enter into the formu-lation of the equations of motion of the train cars [16, 18].

It is, therefore, the objective of this investigation to examine the effect of the coupler inertia on the dynamics and computational efficiency of train models. The results obtained using the two models, inertial and noninertial coupler models, are compared in order to examine the assumption of neglecting the coupler inertia. In the case of the noninertial coupler model, the quasi-static coupler condition used in this investigation do not require having velocity dependent terms as compared to methods previously published in the literature [1]. Only algebraic equations are required in order to be able to use the procedure employed in this study. Nonetheless, velocity dependent forces can still be included in the noninertial coupler formulation used in this paper. A frequency domain analysis is also performed in order to identify the frequencies in the solution associated with the coupler inertia.

3 Inertial and noninertial coordinates

The concept of the inertial and non-inertial coordinates is discussed in this section. Inertial coordinates have generalized inertia forces associated with them, while the noninertial coordinates have no generalized inertia forces. In order to avoid having a singular inertia matrix and/or high frequency oscillations, the second derivatives of the noninertial coordinates are not used when formulating the system equations of motion in this study. In this case, the system coordinates are partitioned into two distinct sets; *inertial* and *noninertial coordinates*, leading to a formulation similar to the one used in the case of nongeneralized coordinates [14]. The use of the principle of virtual work leads to a coupled system of differential and algebraic equations expressed in terms of the inertial and noninertial coordinates. The differential equations are used to determine the inertial accelerations which can be integrated to determine the inertial coordinates and velocities. The noninertial coordinates are determined by using an iterative Newton–Raphson algorithm to solve a set of nonlinear algebraic force equations obtained using quasistatic equilibrium conditions. The noninertial velocities are determined by solving these algebraic force equations at the velocity level. The noninertial coordinates and velocities enter into the formulation of the generalized forces associated with the inertial coordinates.

3.1 Inertial system

If all the coordinates of the bodies in a MBS are treated as inertial coordinates, the equations of motion of a body i can be written as (Roberson and Schertassek [9]; Shabana et al. [15])

$$\mathbf{M}^i \ddot{\mathbf{q}}^i = \mathbf{Q}_e^i + \mathbf{Q}_c^i + \mathbf{Q}_v^i \tag{1}$$

where $\mathbf{M}^i$ is the mass matrix of the body, $\ddot{\mathbf{q}}^i = [\ \ddot{\mathbf{R}}^{iT} \quad \ddot{\boldsymbol{\theta}}^{iT}\ ]^T$ is the vector of the accelerations of the body with $\mathbf{R}^i$ defining the body translation and $\boldsymbol{\theta}^i$ defining the body orientation, $\mathbf{Q}_e^i$ is the vector of external forces, $\mathbf{Q}_c^i$ is the vector of the constraint forces which can be written in terms of Lagrange multipliers $\boldsymbol{\lambda}$ as $\mathbf{Q}_c^i = -\mathbf{C}_{\mathbf{q}^i}^T \boldsymbol{\lambda}$, $\mathbf{C}_{\mathbf{q}^i}$ is the constraint Jacobian matrix associated with the coordinates of body i, and $\mathbf{Q}_v^i$ is the vector of the inertia forces that absorb terms that are quadratic in the velocities [13]. The nonlinear algebraic kinematic constraint equations can be written in the vector form $\mathbf{C}(\mathbf{q}, t) = \mathbf{0}$, where $\mathbf{q}$ is the vector of the system generalized coordinates, and t is time. The constraint equations at the acceleration level can be written as $\mathbf{C}_\mathbf{q}\ddot{\mathbf{q}} = \mathbf{Q}_d$, where $\mathbf{Q}_d$ is a vector that absorbs first derivatives of the coordinates. Using (1) with the constraint equations at the acceleration level, one obtains

$$\begin{bmatrix} \mathbf{M} & \mathbf{C}_\mathbf{q}^T \\ \mathbf{C}_\mathbf{q} & \mathbf{0} \end{bmatrix} \begin{bmatrix} \ddot{\mathbf{q}} \\ \boldsymbol{\lambda} \end{bmatrix} = \begin{bmatrix} \mathbf{Q}_e + \mathbf{Q}_v \\ \mathbf{Q}_d \end{bmatrix} \tag{2}$$

This matrix equation, which ensures that the constraint equations are satisfied at the acceleration level, can be solved for the accelerations and Lagrange multipliers. In order to ensure that the algebraic kinematic constraint equations are satisfied at the position and velocity levels, the independent inertial accelerations $\ddot{\mathbf{q}}_i$ are identified and integrated forward in time in order to determine the independent velocities $\dot{\mathbf{q}}_i$ and independent coordinates $\mathbf{q}_i$. Knowing the independent coordinates from the numerical integration, the dependent coordinates $\mathbf{q}_d$ can be determined from the nonlinear constraint equations using an iterative Newton–Raphson algorithm that requires the solution of the system $\mathbf{C}_{\mathbf{q}_d} \Delta\mathbf{q}_d = -\mathbf{C}$, where $\Delta\mathbf{q}_d$ is the vector of Newton differences, and $\mathbf{C}_{\mathbf{q}_d}$ is the constraint Jacobian matrix associated with the dependent coordinates. Knowing the system coordinates and the independent velocities, the dependent velocities $\dot{\mathbf{q}}_d$ can be determined by solving a linear system of algebraic equations that represents the constraint equations at the velocity level. This linear system of equations in the velocities can be written as $\mathbf{C}_{\mathbf{q}_d}\dot{\mathbf{q}}_d = -\mathbf{C}_{\mathbf{q}_i}\dot{\mathbf{q}}_i - \mathbf{C}_t$; where $\mathbf{C}_{\mathbf{q}_i}$ is the constraint Jacobian matrix associated with the independent coordinates, and $\mathbf{C}_t = \partial\mathbf{C}/\partial t$ is the partial derivative of the constraint functions with respect to time.

Lagrange multipliers, on the other hand, can be used to determine the constraint forces. For a given joint k, the generalized constraint forces acting on body i, connected by this joint, can be obtained from the equation

$$(\mathbf{Q}_c^i)_k = -(\mathbf{C}_k)_{\mathbf{q}^i}^T \boldsymbol{\lambda}_k = \begin{bmatrix} \mathbf{F}_k^{iT} & \mathbf{T}_k^{iT} \end{bmatrix}^T \tag{3}$$

where $\mathbf{F}_k^i$ and $\mathbf{T}_k^i$ are the generalized joint forces associated, respectively, with the translation and orienta-tion coordinates of body i. Using the results of (3), the reaction forces at the joint definition point can be de-termined using the concept of the equipollent system of forces.

3.2 Noninertial coordinates

In developing the augmented form of (2), it is assumed that all coordinates have generalized inertia forces as-sociated with them. In some MBS applications, the inertia associated with some coordinates can be rel-atively small. This can lead to high frequency oscil-lations that have negligible effect on the solution but cause significant deterioration of the computational ef-ficiency. For this reason, it is important to develop a computational procedure that allows for eliminating these high frequency oscillations by neglecting the ef-fect of the small inertia. If the small inertia can be ne-glected, the virtual work of the inertia forces δW_i and the virtual work of the applied forces δW_e can be writ-ten, respectively, as

$$\delta W_i = \mathbf{Q}_i^T \delta \mathbf{q}, \quad \delta W_e = \mathbf{Q}_e^T \delta \mathbf{q} + \mathbf{Q}_{ni}^T \delta \mathbf{q}_{ni} \tag{4}$$

In this equation, $\mathbf{q}$ is the vector of the system inertial coordinates that have inertia forces associated with them, $\mathbf{q}_{ni}$ is the vector of the system non-inertial coordinates which have no inertia forces associated with them, $\mathbf{Q}_i$ is the vector of generalized inertia forces, $\mathbf{Q}_e$ is the vector of generalized applied forces associated with the inertial coordinates, and $\mathbf{Q}_{ni}$ is the vector of generalized applied forces associated with the noninertial coordinates. Using (4) and the principle of virtual work, which states that $\delta W_i = \delta W_e$, one has

$$\mathbf{Q}_{ie}^T \delta \mathbf{q} - \mathbf{Q}_{ni}^T \delta \mathbf{q}_{ni} = \mathbf{0} \tag{5}$$

In this equation, $\mathbf{Q}_{ie} = \mathbf{Q}_i - \mathbf{Q}_e$. If the system is subjected to kinematic constraints that describe specified motion trajectories and mechanical joints, the vector of nonlinear algebraic constraint functions can be written as

$$\mathbf{C}(\mathbf{q}, \mathbf{q}_{ni}, t) = \mathbf{0} \tag{6}$$

Considering a virtual change in the coordinates, one obtains $\mathbf{C}_\mathbf{q} \delta \mathbf{q} + \mathbf{C}_{\mathbf{q}_{ni}} \delta \mathbf{q}_{ni} = \mathbf{0}$. Multiplying this equation by Lagrange multipliers $\boldsymbol{\lambda}$, adding the results to (5), and using the generalized coordinate partitioning as inertial and noninertial, one obtains

$$\mathbf{Q}_{ie} + \mathbf{C}_\mathbf{q}^T \boldsymbol{\lambda} = \mathbf{0}, \quad \mathbf{Q}_{ni} + \mathbf{C}_{\mathbf{q}_{ni}}^T \boldsymbol{\lambda} = \mathbf{0} \tag{7}$$

Differentiating (6) twice with respect to time, one ob-tains the constraint equations at the acceleration level,

$\mathbf{C}_\mathbf{q} \ddot{\mathbf{q}} + \mathbf{C}_{\mathbf{q}_{ni}} \ddot{\mathbf{q}}_{ni} = \mathbf{Q}_d$, where $\mathbf{Q}_d$ is the quadratic velocity vector that arises from the differentiation of the kinematic constraint equations twice with respect to time. By combining the constraint equations at the acceleration level with (7), one obtains

$$\begin{bmatrix} \mathbf{M} & \mathbf{0} & \mathbf{C}_\mathbf{q}^T \\ \mathbf{0} & \mathbf{0} & \mathbf{C}_{\mathbf{q}_{ni}}^T \\ \mathbf{C}_\mathbf{q} & \mathbf{C}_{\mathbf{q}_{ni}} & \mathbf{0} \end{bmatrix} \begin{bmatrix} \ddot{\mathbf{q}} \\ \ddot{\mathbf{q}}_{ni} \\ \boldsymbol{\lambda} \end{bmatrix} = \begin{bmatrix} \mathbf{Q}_e \\ \mathbf{Q}_{ni} \\ \mathbf{Q}_d \end{bmatrix} \tag{8}$$

In the special case in which the noninertial coordinates are not subjected to constraints, the preceding equation leads to

$$\begin{bmatrix} \mathbf{M} & \mathbf{C}_\mathbf{q}^T \\ \mathbf{C}_\mathbf{q} & \mathbf{0} \end{bmatrix} \begin{bmatrix} \ddot{\mathbf{q}} \\ \boldsymbol{\lambda} \end{bmatrix} = \begin{bmatrix} \mathbf{Q}_e \\ \mathbf{Q}_d \end{bmatrix}, \quad \mathbf{Q}_{ni}(\mathbf{q}, \mathbf{q}_{ni}, \dot{\mathbf{q}}, \dot{\mathbf{q}}_{ni}, t) = \mathbf{0} \tag{9}$$

Furthermore, if an embedding technique is used to systematically eliminate the dependent inertial coordinates such that all the components of the vector $\mathbf{q}$ are independent, the preceding equations reduce to

$$\mathbf{M}\ddot{\mathbf{q}} = \mathbf{Q}_e, \quad \mathbf{Q}_{ni}(\mathbf{q}, \mathbf{q}_{ni}, \dot{\mathbf{q}}, \dot{\mathbf{q}}_{ni}, t) = \mathbf{0} \tag{10}$$

The second equation of (10) depends on the coordinates and velocities. The velocity terms appear in this study when coupler damping forces are considered. The procedure developed in this investigation is based on developing a quasistatic equilibrium force conditions that depend on the noninertial coordinates. This leads to a system of nonlinear algebraic equations, rep-resented by the second equation of (10) that can be it-eratively solved, using a Newton–Raphson algorithm, for the noninertial coordinates for given set of iner-tial coordinates. The non-inertial velocities are deter-mined by differentiating the quasistatic algebraic force equations. This procedure is fundamentally different from the procedure presented by Arnold et al. [1] and Burgermeister et al. [3] in which the force equations must include velocity dependent terms and these force equations are treated as first-order ordinary differen-tial equations that are integrated with the equations of motion.

4 Coupler kinematics using redundant coordinates

As previously mentioned, in most coupler models reported in the literature, the coupler is represented using a discrete massless spring-damper element which

has no kinematic degrees of freedom. This simple model does not capture geometric nonlinearities resulting from the relative motion between the coupler components as well as the relative motion of the coupler with respect to the car body. In this investigation, the coupler kinematic degrees of freedom are considered. There are two methods for the description of the coupler kinematics. In the first method, the coupler nonlinear kinematic equations are formulated in terms of redundant coordinates that are related by algebraic constraint equations. This approach is used in most general purpose MBS computer algorithms and it leads to a sparse matrix structure of the equations of motion. Nonetheless, the redundant coordinate approach requires the solution of a system of differential and algebraic equations and the use of the technique of Lagrange multipliers that can be used to determine the generalized constraint forces. In the second approach, the kinematic equations of the coupler are expressed in terms of the coupler degrees of freedom. This approach is more suited for the implementation in longitudinal train force dynamics algorithms which tend to be simpler as compared to general MBS algorithms and do not in general allow for the solution of coupled sets of differential and algebraic equations. Such a coupler model will be discussed in later sections of this study.

In this section, the kinematics using the redundant coordinate approach is discussed. As shown in Fig. 1, the coupler consists of a shank and a draft gear or an End-of-car cushioning (EOC) device unit. The draft gear or EOC device is connected to the car body using a prismatic joint, while the shank is connected to the draft gear or EOC device using a pin joint that allows for the relative rotation of the shank with respect to the car body. The draft gear produces dry friction force, while the EOC device produces viscous damping force; both oppose the sliding motion of the coupler with respect to the car body. In order to have a meaningful comparison between the effects of the two types of forces, the stiffness of the coupler is assumed to be the same for both coupler types. As previously mentioned, in the coupler model considered in this study, the draft gear or end of car cushioning are assumed to be connected to the car body using a prismatic (translational) joint that allows for relative translation along the joint axis. In general MBS algorithms, the nonlinear algebraic equations that define the prismatic joint are expressed in terms of the absolute coordinates of the two bodies i and j connected by the joint. The five algebraic constraint equations that eliminate five degrees of freedom can be written in terms of the absolute Cartesian coordinates of the two bodies as [13].

$$\mathbf{C}(\mathbf{q}^i, \mathbf{q}^j) = \begin{bmatrix} \mathbf{v}_1^{iT}\mathbf{v}^j & \mathbf{v}_2^{iT}\mathbf{v}^j & \mathbf{v}_1^{iT}\mathbf{r}_P^{ij} & \mathbf{v}_2^{iT}\mathbf{r}_P^{ij} & \mathbf{h}^{iT}\mathbf{h}^j \end{bmatrix}^T = \mathbf{0} \tag{11}$$

where $\mathbf{h}^i$ and $\mathbf{h}^j$ are two orthogonal vectors drawn perpendicular to the joint axis, defined respectively on bodies i and j; $\mathbf{v}^i$ and $\mathbf{v}^j$ are two vectors defined along the joint axis on bodies i and j, respectively; $\mathbf{v}^i, \mathbf{v}_1^{iT}, \mathbf{v}_2^{iT}$ form an orthogonal triad defined on body i; and

$$\mathbf{r}_P^{ij} = \mathbf{r}_P^i - \mathbf{r}_P^j = \mathbf{R}^i + \mathbf{A}^i\bar{\mathbf{u}}_P^i - \mathbf{R}^j - \mathbf{A}^j\bar{\mathbf{u}}_P^j \tag{12}$$

In this equation, $\mathbf{A}^i$ and $\mathbf{A}^j$ are the transformation matrices that define the orientation of bodies i and j, respectively; and $\bar{\mathbf{u}}_P^i$ and $\bar{\mathbf{u}}_P^j$ are the local position vectors of points P^i and P^j with respect to bodies i and j, respectively. Points P^i and P^j are defined on the axis of the prismatic joint on bodies i and j, respectively. One can show that the Jacobian matrix of the prismatic joint constraints is defined as

$$\mathbf{C}_\mathbf{q} = [\,\mathbf{C}_{\mathbf{q}^i} \quad \mathbf{C}_{\mathbf{q}^j}\,] = \begin{bmatrix} \mathbf{v}^{jT}\mathbf{H}_1^i & \mathbf{v}_1^{iT}\mathbf{H}^j \\ \mathbf{v}^{jT}\mathbf{H}_2^i & \mathbf{v}_2^{iT}\mathbf{H}^j \\ \mathbf{r}_P^{ijT}\mathbf{H}_1^i + \mathbf{v}_1^{iT}\mathbf{H}_P^i & -\mathbf{v}_1^{iT}\mathbf{H}_P^j \\ \mathbf{r}_P^{ijT}\mathbf{H}_2^i + \mathbf{v}_2^{iT}\mathbf{H}_P^i & -\mathbf{v}_2^{iT}\mathbf{H}_P^j \\ \mathbf{h}^{jT}\mathbf{H}_h^i & \mathbf{h}^{iT}\mathbf{H}_h^j \end{bmatrix} \tag{13}$$

where $\mathbf{C}_{\mathbf{q}^i}$ and $\mathbf{C}_{\mathbf{q}^j}$ are the constraint Jacobian matrices associated with the coordinates of bodies i and j, respectively; and other vectors and matrices that appear in the preceding equation are

$$\mathbf{H}_P^i = \begin{bmatrix} \mathbf{I} & \mathbf{A}^i\tilde{\bar{\mathbf{u}}}_P^{iT}\bar{\mathbf{G}}^i \end{bmatrix}, \quad \mathbf{H}_P^j = \begin{bmatrix} \mathbf{I} & \mathbf{A}^j\tilde{\bar{\mathbf{u}}}_P^{jT}\bar{\mathbf{G}}^j \end{bmatrix},$$

$$\mathbf{H}_1^i = \frac{\partial \mathbf{v}_1^i}{\partial \mathbf{q}^i} = \frac{\partial}{\partial \mathbf{q}^i}\left(\mathbf{A}^i\bar{\mathbf{v}}_1^i\right), \quad \mathbf{H}_2^i = \frac{\partial \mathbf{v}_2^i}{\partial \mathbf{q}^i} = \frac{\partial}{\partial \mathbf{q}^i}\left(\mathbf{A}^i\bar{\mathbf{v}}_2^i\right),$$

$$\mathbf{H}^j = \frac{\partial \mathbf{v}^j}{\partial \mathbf{q}^j} = \frac{\partial}{\partial \mathbf{q}^j}\left(\mathbf{A}^j\bar{\mathbf{v}}^j\right), \quad \mathbf{H}_h^i = \begin{bmatrix} \mathbf{0} & \mathbf{A}^i\tilde{\bar{\mathbf{h}}}^{iT}\bar{\mathbf{G}}^i \end{bmatrix},$$

and

$$\mathbf{H}_h^j = \begin{bmatrix} \mathbf{0} & \mathbf{A}^j\tilde{\bar{\mathbf{h}}}^{jT}\bar{\mathbf{G}}^j \end{bmatrix}$$

In these equations, $\tilde{\bar{\mathbf{h}}}$ is the skew symmetric matrix associated with the vector $\bar{\mathbf{h}}$.

The shank of the coupler is assumed to be connected to the draft gear or EOC device using a pin joint. In this model, only one relative rotation degree of freedom about the Z axis is considered [5]. In the case of the pin joint, the algebraic constraint equations in terms of the absolute Cartesian coordinates are the same as the equations of the prismatic joint given by (11) except of replacing the last equation by the constraint equation $\mathbf{r}_P^{ijT}\mathbf{r}_P^{ij} - k_\theta = 0$, where k_θ is a constant [13], and $\mathbf{r}_P^{ij} = \mathbf{r}^i{}_P - \mathbf{r}^j{}_P$. Using the algebraic constraint equations of the pin joint, one can show that the Jacobian matrix of the revolute joint constraints can be written as

$$\mathbf{C}_\mathbf{q} = [\,\mathbf{C}_{\mathbf{q}^i} \quad \mathbf{C}_{\mathbf{q}^j}\,] = \begin{bmatrix} \mathbf{v}^{jT}\mathbf{H}_1^i & \mathbf{v}_1^{iT}\mathbf{H}^j \\ \mathbf{v}^{jT}\mathbf{H}_2^i & \mathbf{v}_2^{iT}\mathbf{H}^j \\ \mathbf{r}_P^{ijT}\mathbf{H}_1^i + \mathbf{v}_1^{iT}\mathbf{H}_P^i & -\mathbf{v}_1^{iT}\mathbf{H}_P^j \\ \mathbf{r}_P^{ijT}\mathbf{H}_2^i + \mathbf{v}_2^{iT}\mathbf{H}_P^i & -\mathbf{v}_2^{iT}\mathbf{H}_P^j \\ 2\mathbf{r}_P^{ijT}\mathbf{H}_P^i & -2\mathbf{r}_P^{ijT}\mathbf{H}_P^j \end{bmatrix} \tag{14}$$

where the vectors and matrices that appear in this equation are the same as previously defined in this section.

5 Coupler force equations and algorithm

In this section, the formulations of the forces resulting from the connection between the car body and shank with the draft gear or EOC device; and the forces resulting from the coupler knuckle connection are presented. The generalized forces associated with the absolute Cartesian coordinates that are used in general MBS algorithms are obtained. The computational algorithm used with the redundant coordinate formulation is also summarized before concluding this section in order to shed light on the fundamental differences between general MBS algorithms used in this investigation for developing the inertial coupler model and the simpler LTD algorithms used for developing the noninertial coupler model. While linear stiffness and damping coefficients are used in this investigation, nonlinear coefficients obtained using measurements can also be considered using a spline function representation.

5.1 Draft gear/EOC connection

The car body is assumed to be connected to the draft gear or EOC device using a compliant force element that has stiffness k_B and damping coefficient c_B. The force due to this compliant force element can be written as

$$F_B = k_B(l - l_0) + c_B\dot{l} \tag{15}$$

where l is the current spring length, l_0 is the initial spring length, and $\dot{l}$ is the time rate of deformation of the spring. Using the virtual work, $\delta W = -F_B\delta l$, and the definition of l as $l = \sqrt{\mathbf{r}_B^{ijT}\mathbf{r}_B^{ij}}$, where i and j refer to the two components connected by the spring, one can write the virtual change in the spring length in terms of the virtual changes in the absolute Cartesian coordinates as

$$\delta l = \left(\mathbf{r}_B^{ijT}\mathbf{r}_B^{ij}\right)^{-1/2}\mathbf{r}_B^{ijT}\delta\mathbf{r}_B^{ij} = \frac{1}{l}\mathbf{r}_B^{ijT}\delta\mathbf{r}_B^{ij} = \frac{\mathbf{r}_B^{ijT}}{l}\left[\delta\mathbf{R}^i - \tilde{\mathbf{u}}_B^i\mathbf{G}^i\delta\boldsymbol{\theta}^i - \delta\mathbf{R}^j + \tilde{\mathbf{u}}_B^j\mathbf{G}^j\delta\boldsymbol{\theta}^j\right] \tag{16}$$

where $\mathbf{r}_B^{ij} = \mathbf{r}_B^i - \mathbf{r}_B^j$ defines the position vector of the spring attachment point B^i on the draft gear or EOC device with respect to the spring attachment point B^j on the car body; $\mathbf{G}^i$ and $\mathbf{G}^j$ are the matrices that relate the angular velocity vector to the derivatives of the orientation parameters; $\tilde{\mathbf{u}}_B^i$ and $\tilde{\mathbf{u}}_B^j$ are the skew symmetric matrices associated with the vectors $\mathbf{A}^i\bar{\mathbf{u}}_B^i$ and $\mathbf{A}^j\bar{\mathbf{u}}_B^j$ that define the locations of the spring attachment points with respect to the origin of the coordinate systems of bodies i and j, respectively; and $\mathbf{A}^i$ and $\mathbf{A}^j$ are the transformation matrices that define the orientation of the two bodies. Defining the direction of the force F_B by the unit vector $\hat{\mathbf{r}}_B^{ij} = \mathbf{r}_B^{ij}/l$, the virtual work can be written as

$$\delta W = -F_B\hat{\mathbf{r}}_B^{ijT}\left[\delta\mathbf{R}^i - \tilde{\mathbf{u}}_B^i\mathbf{G}^i\delta\boldsymbol{\theta}^i - \delta\mathbf{R}^j + \tilde{\mathbf{u}}_B^j\mathbf{G}^j\delta\boldsymbol{\theta}^j\right] = \mathbf{Q}_R^{iT}\delta\mathbf{R}^i + \mathbf{Q}_\theta^{iT}\delta\boldsymbol{\theta}^i + \mathbf{Q}_R^{jT}\delta\mathbf{R}^j + \mathbf{Q}_\theta^{jT}\delta\boldsymbol{\theta}^j \tag{17}$$

which can be rewritten in a compact form as $\delta W = \mathbf{Q}_B^{iT}\delta\mathbf{q}^i + \mathbf{Q}_B^{jT}\delta\mathbf{q}^j$, where $\mathbf{q}^i$ and $\mathbf{q}^j$ are the generalized coordinates of bodies i and j, and

$$\mathbf{Q}_B^i = \begin{bmatrix} \mathbf{Q}_R^i \\ \mathbf{Q}_\theta^i \end{bmatrix} = \begin{bmatrix} -F_B\hat{\mathbf{r}}_B^{ij} \\ F_B\mathbf{G}^{iT}\tilde{\mathbf{u}}_B^{iT}\hat{\mathbf{r}}_B^{ij} \end{bmatrix},$$

$$\mathbf{Q}_B^j = \begin{bmatrix} \mathbf{Q}_R^j \\ \mathbf{Q}_\theta^j \end{bmatrix} = \begin{bmatrix} F_B \hat{\mathbf{r}}_B^{ij} \\ -F_B \mathbf{G}^{jT} \tilde{\mathbf{u}}_B^{jT} \hat{\mathbf{r}}_B^{ij} \end{bmatrix} \tag{18}$$

This equation defines the generalized forces associated with the absolute Cartesian coordinates due to the connection of the draft gear or EOC device with the car body.

5.2 Shank connection

In this investigation, the shank is assumed to be connected to the draft gear or EOC device by a pin joint which allows yaw rotation. The restoring torque resulting from the relative shank rotation is introduced using a rotational spring-damper element. This torque is assumed to take the following form:

$$T^{ij} = k_r \theta^{ij} + c_r \dot{\theta}^{ij} \tag{19}$$

where θ^{ij} represents the relative rotation of the shank. The virtual change in this rotation can be defined as

$$\delta\theta^{ij} = \mathbf{h}^{ijT} \left(\mathbf{G}^i \delta\boldsymbol{\theta}^i - \mathbf{G}^j \delta\boldsymbol{\theta}^j \right) \tag{20}$$

where $\mathbf{G}^i$ and $\mathbf{G}^j$ are as defined before, and $\mathbf{h}^{ij}$ is a unit vector along the joint axis. Using the virtual work, one has

$$\delta W = -T^{ij} \delta\theta^{ij} = \mathbf{Q}_r^{iT} \delta\mathbf{q}^i + \mathbf{Q}_r^{jT} \delta\mathbf{q}^j \tag{21}$$

where $\mathbf{Q}_r^i = [\mathbf{0} \quad -(T^{ij} \mathbf{G}^{iT} \mathbf{h}^{ij})^T]^T$, and $\mathbf{Q}_r^j = [\mathbf{0} \quad (T^{ij} \mathbf{G}^{jT} \mathbf{h}^{ij})^T]^T$.

These generalized forces are nonlinear functions of the relative shank rotation.

5.3 Knuckle force model

The connection between the couplers of two cars is represented by a compliant element that define the knuckle force model. Following a procedure similar to the one used previously in this section, one can define the following vectors of generalized forces associated with the absolute Cartesian coordinates of the shanks of the two couplers that connect two cars:

$$\mathbf{Q}_{rr}^i = \begin{bmatrix} \mathbf{Q}_R^i \\ \mathbf{Q}_\theta^i \end{bmatrix} = \begin{bmatrix} -F_Q \hat{\mathbf{r}}_Q^{ij} \\ F_Q \mathbf{G}^{iT} \tilde{\mathbf{u}}_Q^{iT} \hat{\mathbf{r}}_Q^{ij} \end{bmatrix},$$

$$\mathbf{Q}_{rr}^i = \begin{bmatrix} \mathbf{Q}_R^j \\ \mathbf{Q}_\theta^j \end{bmatrix} = \begin{bmatrix} F_Q \hat{\mathbf{r}}_Q^{ij} \\ -F_Q \mathbf{G}^{jT} \tilde{\mathbf{u}}_Q^{jT} \hat{\mathbf{r}}_Q^{ij} \end{bmatrix} \tag{22}$$

where the force is defined as

$$F_Q = k_{rr} l_{rr} + c_{rr} \dot{l}_{rr} \tag{23}$$

and k_{rr} and c_{rr} are, respectively, the stiffness and damping coefficients of the knuckle; l_{rr} is the relative displacement between the two shanks; and $\dot{l}_{rr}$ is the rate of the relative displacement.

5.4 Solution algorithm

The inertial coupler model is developed using a general MBS algorithm based on the redundant coordinates. The dynamic equations of motion of the train system are augmented with the nonlinear algebraic equations that describe mechanical joints and specified motion trajectories. These algebraic equations are satisfied at the position, velocity, and acceleration levels. As previously mentioned, LTD algorithms tend to be much simpler than general MBS algorithms that require the use of a procedure for the solution of differential and algebraic equations. The simpler LTD algorithms will be discussed in later sections of this paper.

General MBS algorithms employ the technique of Lagrange multipliers and they are, for the most part, based on (2). These algorithms also exploit sparse matrix techniques in order to obtain efficient solution for the nonlinear dynamic equations of motion. Using the developments presented in Sect. 2, the following algorithm is used for developing the inertial coupler model:

1. An estimate of the initial conditions that define the initial configuration of the MBS is made. The initial conditions that represent the initial coordinates and velocities must be a good approximation of the exact initial configuration.
2. Using the initial coordinates, the constraint Jacobian matrix $\mathbf{C_q}$ can be constructed, and based on the numerical structure of this matrix an LU factorization algorithm can be used to identify a set of independent coordinates.
3. Using the values of the independent coordinates, the constraint equations $\mathbf{C}(\mathbf{q}, t) = \mathbf{0}$ can be considered as a nonlinear system of algebraic equations in the dependent coordinates. This system can be solved iteratively using a Newton–Raphson algorithm and sparse matrix techniques.
4. Assuming that the independent coordinates and velocities are known from the numerical integration

and the dependent coordinates are determined from the previous step, one can construct the constraint equations at the velocity level, $\mathbf{C_q}\dot{\mathbf{q}} = -\mathbf{C}_t$, where $\mathbf{C}_t$ is the partial derivative of the constraint functions with respect to time. This linear system of algebraic equations has a number of scalar equations equal to the number of dependent velocities.

5. Having determined the coordinates and velocities, (2) can be constructed and solved for the accelerations and Lagrange multipliers. The vector of Lagrange multipliers can be used to determine the generalized reaction forces.
6. The independent accelerations can be identified and used to define the state space equations which can be integrated forward in time using a direct numerical integration method. The numerical solution of the state equations defines the independent coordinates and velocities, which can be used to determine the dependent coordinates and velocities as discussed in steps 3 and 4.
7. This process continues until the desired end of the simulation time is reached.

The solution algorithm used for developing the noninertial coupler model differs significantly from the solution algorithm discussed in this section as will be explained in later sections of this paper. Nonetheless, both algorithms require the solution of differential and algebraic equations. The algebraic equations in the case of the noninertial coupler model, however, are obtained from force equations instead of kinematic constraint equations.

6 Longitudinal train dynamics (LTD)

Specialized LTD algorithms tend to be simpler as compared to general MBS algorithms. LTD algorithms do not in general require the solution of DAE's system and are based on formulations that employ independent coordinates. They are designed to solve efficiently long train consists for the purpose of analyzing the longitudinal forces acting on the consist cars. These longitudinal forces can include tractive, braking, resistance, and coupler forces. Efficient implementation of some of these force elements such as couplers may require modifying LTD algorithms to allow for solving algebraic equations simultaneously with the system equations of motion. As previously mentioned, the implementation of efficient coupler models may require the neglect of the coupler inertia leading to noninertial coordinates that can be determined by solving a system of algebraic equations obtained using a quasistatic force analysis [16]. In this section, the kinematic equations of the coupler are developed in terms of independent relative coordinates in order to allow for a systematic implementation in LTD algorithms.

6.1 Draft gear/EOC connection

The slider block B^i, shown in Fig. 3, can represent a draft gear or EOC device. The global position vector of the center of this block, which slides with respect to the car body i, can be written as

$$\mathbf{r}^i_B = \mathbf{R}^i + \mathbf{A}^i\left(\bar{\mathbf{u}}^i_{Po} + \bar{\mathbf{u}}^i_d\right) - \left(\left(\mathbf{R}^i - \mathbf{R}^i_o\right)^T \hat{\mathbf{d}}^i_B\right)\hat{\mathbf{d}}^i_B \quad (24)$$

In this equation, $\mathbf{R}^i$ is the global position vector of the origin of the coordinate system of car body i, $\mathbf{A}^i$ is the transformation matrix that defines the orientation of the coordinate system of car body i, $\bar{\mathbf{u}}^i_{Po}$ is the local position vector of point P^i, $\bar{\mathbf{u}}^i_d = (l^i_o + d^i)\hat{\bar{\mathbf{d}}}^i_B$, $\hat{\bar{\mathbf{d}}}^i_B$ is a unit vector that defines the block sliding axis, l^i_o is the initial distance between point P^i and the center of the block B^i, $\hat{\mathbf{d}}^i_B = \mathbf{A}^i\hat{\bar{\mathbf{d}}}^i_B$, $\mathbf{R}^i_o$ is the global position of the origin of the car body coordinate system before displacement, and d^i is the distance that measures the location of the block along $\hat{\bar{\mathbf{d}}}^i_B$. Due to the fact that d^i in (24) is defined as $d^i = d^i_d + (\mathbf{R}^i - \mathbf{R}^i_o)^T\,\hat{\mathbf{d}}^i_B$, where d^i_d is the relative displacement of the sliding block with respect to the car body i, the last term in (24) is introduced to eliminate the effect of the translation
of the car body in the direction of $\hat{\mathbf{d}}^i_B$ on the displacement of the slider block. The virtual displacement of the position vector of (24) can then be written as

$$\begin{aligned}\delta\mathbf{r}^i_B &= \delta\mathbf{R}^i - \mathbf{A}^i\left(\tilde{\bar{\mathbf{u}}}^i_o + \tilde{\bar{\mathbf{u}}}^i_d\right)\bar{\mathbf{G}}^i\delta\boldsymbol{\theta}^i + \mathbf{A}^i\hat{\bar{\mathbf{d}}}^i_B\delta d^i \\ &\quad + \mathbf{L}^i_{Rd}\delta\mathbf{q}^i \\ &= \left(\mathbf{L}^i_B + \mathbf{L}^i_{Rd}\right)\delta\mathbf{q}^i + \mathbf{L}^i_{Bd}\delta d^i \end{aligned} \quad (25)$$

where

$$\left.\begin{aligned}&\mathbf{L}^i_B = \left[\mathbf{I} \quad -\mathbf{A}^i\left(\tilde{\bar{\mathbf{u}}}^i_{P0} + \tilde{\bar{\mathbf{u}}}^i_d\right)\bar{\mathbf{G}}^i\right], \\ &\mathbf{L}^i_{Bd} = \mathbf{A}^i\hat{\bar{\mathbf{d}}}^i_B, \\ &\mathbf{L}^i_{Rd} = \left[-\left(\hat{\mathbf{d}}^i_B \otimes \hat{\mathbf{d}}^i_B\right) \quad 2\left(\left(\mathbf{R}^i - \mathbf{R}^i_o\right)^T\hat{\mathbf{d}}^i_B\right)\mathbf{A}^i\hat{\bar{\mathbf{d}}}^i_B\bar{\mathbf{G}}^i\right]\end{aligned}\right\} \quad (26)$$

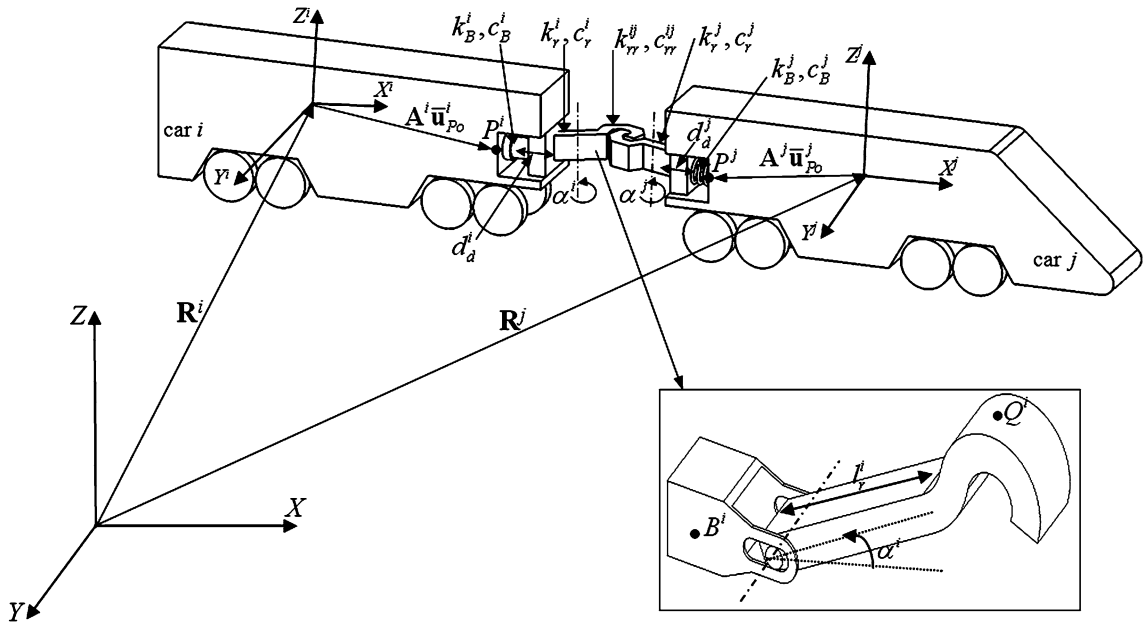

Fig. 3 Two-car system

The kinematic equations of the slider block will be used to define the draft gear and EOC kinematics.

6.2 Shank rotation

As shown in Fig. 3, the shank is subjected to a base motion defined by the sliding d_d^i and is allowed to ro-tate by the angle α^i with respect to the car body. The location of the end point Q^i of the shank with respect to the origin of the car body coordinate system is de-fined by the vector $\mathbf{u}^{-i}{}_Q = \mathbf{u}^{-i}{}_{P0} + \bar{\mathbf{u}}^i{}_d + \mathbf{u}^{-i}{}_r$, where as shown in Fig. 3, $\mathbf{u}^{-i}{}_r$ is a vector defined along the rotating arm which is assumed to have length l_r^i. It follows that

$$\bar{\mathbf{u}}_r^i = l_r^i\begin{bmatrix}\cos\alpha^i & \sin\alpha^i & 0\end{bmatrix}^T \tag{27}$$

One can then write the global position vector of point Q^i shown in Fig. 3 as

$$\mathbf{r}_Q^i = \mathbf{R}^i + \mathbf{A}^i\bar{\mathbf{u}}_Q^i - \left(\left(\mathbf{R}^i - \mathbf{R}_o^i\right)^T\hat{\mathbf{d}}_B^i\right)\hat{\mathbf{d}}_B^i \tag{28}$$

The virtual change in this position vector can be written as

$$\delta\mathbf{r}_Q^i = \left(\mathbf{L}_Q^i + \mathbf{L}_{Rd}^i\right)\delta\mathbf{q}^i + \mathbf{L}_{Bd}^i\delta d^i + \mathbf{L}_r^i\delta\alpha^i \tag{29}$$

where

$$\mathbf{L}_Q^i = \begin{bmatrix}\mathbf{I} & -\mathbf{A}^i\tilde{\bar{\mathbf{u}}}_Q^i\bar{\mathbf{G}}^i\end{bmatrix}, \quad \mathbf{L}_r^i = \mathbf{A}^i\left(\bar{\mathbf{u}}_r^i\right)_{\alpha^i} \tag{30}$$

In this equation $(\bar{\mathbf{u}}_r^i)_{\alpha^i} = l_r^i[-\sin\alpha^i \quad \cos\alpha^i \quad 0]^T$.

7 LTD noninertial generalized forces

By neglecting the effect of the inertia of the coupler components, one can develop a quasistatic equilibrium conditions that define a set of nonlinear algebraic equations that can be solved for the noninertial coupler coordinates. These nonlinear equations can be solved iteratively using a Newton–Raphson algorithm to determine the noninertial coordinates d_d^i and α^i introduced in the preceding section.

7.1 Coupler forces

The compliant force element that connects the car body i and the draft gear or EOC device is denoted as $\mathbf{f}_B^i$. Similarly, the force associated with car body j is denoted as $\mathbf{f}_B^j$. The forces $\mathbf{f}_B^i$ and $\mathbf{f}_B^j$ can be written as

$$\left.\begin{aligned}\mathbf{f}_B^i &= \left(k_B^i d_d^i + c_B^i\dot{d}_d^i\right)\hat{\mathbf{d}}_B^i,\\ \mathbf{f}_B^j &= \left(k_B^j d_d^j + c_B^j\dot{d}_d^j\right)\hat{\mathbf{d}}_B^j\end{aligned}\right\} \tag{31}$$

In this equation, k_B^i, k_B^j, c_B^i, and c_B^j are the stiffness and damping coefficients associated with the draft gear or EOC of car bodies i and j, respectively. Note that the spring deformations d_d^i and d_d^j can be expressed in terms of d^i and d^j. The virtual work of the forces given in the preceding equation can be written as $\delta W_B^{ij} = \mathbf{f}_B^{iT}\delta\mathbf{r}_P^i - \mathbf{f}_B^{iT}\delta\mathbf{r}_B^i + \mathbf{f}_B^{jT}\delta\mathbf{r}_P^j - \mathbf{f}_B^{jT}\delta\mathbf{r}_B^j$. Using this equation and the expressions of the virtual displacements, one obtains

$$\delta W_B^{ij} = \mathbf{Q}_B^{iT}\delta\mathbf{q}^i + \mathbf{Q}_B^{jT}\delta\mathbf{q}^j + \left(\mathbf{Q}_B^{ij}\right)_{ni}^T\delta\mathbf{q}_{ni}^{ij} \tag{32}$$

In this equation, $\mathbf{q}_{ni}^{ij}$ is the vector of the coupler noninertial coordinates defined as

$$\mathbf{q}_{ni}^{ij} = \begin{bmatrix} d_d^i & \alpha^i & d_d^j & \alpha^j \end{bmatrix}^T \tag{33}$$

and

$$\left.\begin{aligned} \mathbf{Q}_B^i &= \left(\mathbf{L}_P^i - \mathbf{L}_B^i - \mathbf{L}_{Rd}^i\right)^T\mathbf{f}_B^i, \\ \mathbf{Q}_B^j &= \left(\mathbf{L}_P^j - \mathbf{L}_B^j - \mathbf{L}_{Rd}^j\right)^T\mathbf{f}_B^j, \\ \left(\mathbf{Q}_B^{ij}\right)_{ni} &= \begin{bmatrix} -\mathbf{L}_{Bd}^{iT}\mathbf{f}_B^i & 0 & -\mathbf{L}_{Bd}^{jT}\mathbf{f}_B^j & 0 \end{bmatrix}^T \end{aligned}\right\} \tag{34}$$

In order to account for the stiffness at the joint between the coupler shank and the draft gear/EOC of each car, a torsional spring with stiffness k_r^i and damping c_r^i is introduced at this joint. Let $\hat{\mathbf{d}}_r^i$ and $\hat{\mathbf{d}}_r^j$ be unit vectors along the shank and draft gear/EOC joint axis of car bodies i and j, respectively. It follows that the generalized forces associated with the noninertial coordinates α^i and α^j can be written, respectively, as

$$\left.\begin{aligned} Q_r^i &= -k_r^i\left(\alpha^i - \alpha_o^i\right) - c_r^i\dot{\alpha}^i, \\ Q_r^j &= -k_r^j\left(\alpha^j - \alpha_o^j\right) - c_r^j\dot{\alpha}^j \end{aligned}\right\} \tag{35}$$

This leads to the following generalized force vector associated with the noninertial coupler coordinates

$$\left(\mathbf{Q}_r^i\right)_{ni} = \begin{bmatrix} 0 & Q_r^i & 0 & Q_r^j \end{bmatrix}^T \tag{36}$$

The force at the knuckle due to the interaction between the two couplers that connect the two cars is denoted as $\mathbf{f}_{rr}^{ij}$. This force vector can be written as

$$\mathbf{f}_{rr}^{ij} = \left(k_{rr}^{ij}\left(l_r^{ij} - l_{ro}^{ij}\right) + c_{rr}^{ij}\dot{l}_r^{ij}\right)\hat{\mathbf{d}}_{rr}^{ij} \tag{37}$$

In this equation, k_{rr}^{ij} and c_{rr}^{ij} are the spring stiffness and damping coefficients, l_r^{ij} is the current spring length, l_{ro}^{ij} is the un-deformed length of the spring, and $\hat{\mathbf{d}}_{rr}^{ij}$ is a unit vector along the line connecting points Q^i and Q^j, that is, $\hat{\mathbf{d}}_{rr}^{ij} = (\mathbf{r}_Q^i - \mathbf{r}_Q^j)/|\mathbf{r}_Q^i - \mathbf{r}_Q^j|$. The virtual work of the force $\mathbf{f}_{rr}^{ij}$ can be written as $\delta W_{rr}^{ij} = -\mathbf{f}_{rr}^{ijT}\delta\mathbf{r}_Q^i + \mathbf{f}_{rr}^{ijT}\delta\mathbf{r}_Q^j$. This equation upon using the kinematic equations previously developed in this study can be written as

$$\delta W_{rr}^{ij} = \mathbf{Q}_{rr}^{iT}\delta\mathbf{q}^i + \mathbf{Q}_{rr}^{jT}\delta\mathbf{q}^j + \left(\mathbf{Q}_{rr}^{ij}\right)_{ni}^T\delta\mathbf{q}_{ni}^{ij} \tag{38}$$

In this equation,

$$\left.\begin{aligned} \mathbf{Q}_{rr}^i &= -\left(\mathbf{L}_Q^i + \mathbf{L}_{Rd}^i\right)^T\mathbf{f}_{rr}^{ij}, \\ \mathbf{Q}_{rr}^j &= \left(\mathbf{L}_Q^j + \mathbf{L}_{Rd}^j\right)^T\mathbf{f}_{rr}^{ij}, \\ \left(\mathbf{Q}_{rr}^{ij}\right)_{ni} &= \begin{bmatrix} -\mathbf{L}_{Bd}^{iT}\mathbf{f}_{rr}^{ij} & -\mathbf{L}_r^{iT}\mathbf{f}_{rr}^{ij} \\ \mathbf{L}_{Bd}^{jT}\mathbf{f}_{rr}^{ij} & \mathbf{L}_r^{jT}\mathbf{f}_{rr}^{ij} \end{bmatrix}^T \end{aligned}\right\} \tag{39}$$

7.2 Generalized inertial and noninertial forces

Using the expressions of the forces developed in this section, the generalized coupler forces associated with the inertial coordinates of the car bodies i and j can be written as

$$\left.\begin{aligned} \mathbf{Q}_c^i &= \mathbf{Q}_B^i + \mathbf{Q}_{rr}^i = \left(\mathbf{L}_P^i - \mathbf{L}_B^i - \mathbf{L}_{Rd}^i\right)^T\mathbf{f}_B^i \\ &\quad - \left(\mathbf{L}_Q^i + \mathbf{L}_{Rd}^i\right)^T\mathbf{f}_{rr}^{ij}, \\ \mathbf{Q}_c^j &= \mathbf{Q}_B^j + \mathbf{Q}_{rr}^j = \left(\mathbf{L}_P^j - \mathbf{L}_B^j - \mathbf{L}_{Rd}^j\right)^T\mathbf{f}_B^j \\ &\quad + \left(\mathbf{L}_Q^j + \mathbf{L}_{Rd}^j\right)^T\mathbf{f}_{rr}^{ij} \end{aligned}\right\} \tag{40}$$

The forces associated with the noninertial coupler coordinates are

$$\begin{aligned} \left(\mathbf{Q}_c^i\right)_{ni} &= \left(\mathbf{Q}_B^i\right)_{ni} + \left(\mathbf{Q}_{rr}^i\right)_{ni} + \left(\mathbf{Q}_r^i\right)_{ni} \\ &= \begin{bmatrix} -\mathbf{L}_{Bd}^{iT}(\mathbf{f}_B^i + \mathbf{f}_{rr}^{ij}) \\ -\mathbf{L}_r^{iT}\mathbf{f}_{rr}^{ij} + Q_r^i \\ -\mathbf{L}_{Bd}^{jT}(\mathbf{f}_B^j - \mathbf{f}_{rr}^{ij}) \\ \mathbf{L}_r^{jT}\mathbf{f}_{rr}^{ij} + Q_r^j \end{bmatrix} \end{aligned} \tag{41}$$

The generalized forces associated with the car body inertial coordinates of (40) can be introduced to the dynamic equations of motion, while the four-dimensional force vector associated with the coupler noninertial coordinates can be used to solve for the noninertial coordinates d_d^i, α^i, d_d^j, and α^j using an iterative procedure described in the following section.

8 LTD noninertial coupler solution algorithm

As previously mentioned, most LTD algorithms tend to be simpler and do not include a procedure for solving DAE systems. If the inertia of the coupler is neglected, however, (41) can be used to define quasistatic equilibrium conditions of the coupler as $(\mathbf{Q}_c^i)_{ni} = \mathbf{0}$. This vector equation includes, for each coupler connection, four nonlinear scalar equations that can be solved for the noninertial coupler coordinates d_d^i, α^i, d_d^j, and α^j, assuming that the inertial coordinates and velocities are known from the numerical integration of the train dynamic equations of motion. Therefore, when noninertial coupler models are considered in LTD studies, the resulting differential and algebraic equations must be solved simultaneously.

The LTD algorithm used in this investigation, which is implemented in the computer code ATTIF, is based on the trajectory coordinate formulation. The nonlinear train equations of motion are automatically generated in ATTIF and are solved using direct numerical integration method in order to determine the inertial coordinates and velocities. Knowing the inertial coordinates and velocities, the coupler quasistatic equilibrium conditions can be solved iteratively using a Newton–Raphson algorithm in order to determine the noninertial coordinates that enter into the formulation of the generalized forces associated with the train inertial coordinates. In developing the quasistatic algebraic equations used in this investigation, the effect of the noninertial velocities is neglected, leading to a nonlinear system of algebraic equations expressed in terms of the noninertial coordinates. The noninertial velocities are determined by solving the algebraic equations at the velocity level. The steps of the numerical algorithm used in this investigation to solve the resulting DAE system can be summarized as follows:

1. For a given set of initial conditions $\mathbf{q}_0$ and $\dot{\mathbf{q}}_0$ associated with the train inertial coordinates, the quasistatic equilibrium conditions of each cou-pler element are used to define (41). This equa-tion is used to define the train system quasistatic coupler conditions which can be written as $\mathbf{Q}_{ni}(\mathbf{q}, \mathbf{q}_{ni}, \dot{\mathbf{q}}, \dot{\mathbf{q}}_{ni}, t) = \mathbf{0}$, where $\mathbf{q}_{ni}$ is the vector of system noninertial coordinates. If this system de-pends on the noninertial velocities, the effect of the velocities is neglected, thereby defining the system of algebraic equations $\mathbf{Q}_{ni}(\mathbf{q}, \mathbf{q}_{ni}, t) = \mathbf{0}$, where $\mathbf{q}$ and $\dot{\mathbf{q}}$ are assumed to be known from the initial conditions or the numerical integration of the equations of motion.
2. Given the inertial coordinates and velocities $\mathbf{q}$ and $\dot{\mathbf{q}}$, the system $\mathbf{Q}_{ni}(\mathbf{q}, \mathbf{q}_{ni}, t) = \mathbf{0}$ can be solved for $\mathbf{q}_{ni}$ using a Newton–Raphson algorithm that iteratively solves the following system of equations:

$$\frac{\partial \mathbf{Q}_{ni}}{\partial \mathbf{q}_{ni}} \Delta \mathbf{q}_{ni} = -\mathbf{Q}_{ni}(\mathbf{q}, \mathbf{q}_{ni}, t) \tag{42}$$

   In this equation, $\Delta \mathbf{q}_{ni}$ is the vector of Newton differences. Convergence is achieved if the norm of $\Delta \mathbf{q}_{ni}$ or the norm of $\mathbf{Q}_{ni}$ is smaller than a specified tolerance.
3. If the vector $\mathbf{Q}_e$ is function of the noninertial velocities, that is, $\mathbf{Q}_e = \mathbf{Q}_e(\mathbf{q}, \mathbf{q}_{ni}, \dot{\mathbf{q}}, \dot{\mathbf{q}}_{ni}, t)$; an approximate solution for the noninertial velocities can be obtained by differentiating the system $\mathbf{Q}_{ni}(\mathbf{q}, \mathbf{q}_{ni}, t) = \mathbf{0}$ to define the following linear system in the noninertial velocities:

$$\frac{\partial \mathbf{Q}_{ni}}{\partial \mathbf{q}_{ni}} \dot{\mathbf{q}}_{ni} = -\frac{\partial \mathbf{Q}_{ni}}{\partial \mathbf{q}} \dot{\mathbf{q}} - \frac{\partial \mathbf{Q}_{ni}}{\partial t} \tag{43}$$

   The solution of this system can be used to determine the noninertial velocities $\dot{\mathbf{q}}_{ni}$. In obtaining (43), an assumption is made that the inertial coordinates and velocities are assumed to be known.
4. Knowing the inertial coordinates and velocities and the noninertial coordinates and velocities from the previous two steps, the first equation of (10), $\mathbf{M}\ddot{\mathbf{q}} = \mathbf{Q}_e(\mathbf{q}, \mathbf{q}_{ni}, \dot{\mathbf{q}}, \dot{\mathbf{q}}_{ni}, t)$, can be constructed and solved for the inertial accelerations $\ddot{\mathbf{q}}$.
5. The inertial accelerations $\ddot{\mathbf{q}}$ can be integrated forward in time using direct numerical integration method in order to determine the inertial coordinates $\mathbf{q}$ and the inertial velocities $\dot{\mathbf{q}}$.
6. The simulation stops if the end time is reached; otherwise the procedure is repeated starting with Step 2.

In order to solve for the noninertial coordinates, the coefficient matrix in (42) must be evaluated. The evaluation of this matrix requires the following deriva-

tives:

$$\left.\begin{aligned}
&\frac{\partial \mathbf{L}_r^i}{\partial \mathbf{q}_{ni}^{ij}} = [\mathbf{0} \quad -\mathbf{u}_r^i \quad \mathbf{0} \quad \mathbf{0}],\ \frac{\partial \mathbf{L}_r^j}{\partial \mathbf{q}_{ni}^{ij}} = [\mathbf{0} \quad \mathbf{0} \quad \mathbf{0} \quad -\mathbf{u}_r^j],\\
&\frac{\partial \mathbf{d}_{rr}^{ij}}{\partial \mathbf{q}_{ni}^{ij}} = [\hat{\mathbf{d}}_B^i \quad \mathbf{L}_r^i \quad -\hat{\mathbf{d}}_B^j \quad -\mathbf{L}_r^j],\ \frac{\partial l_r^{ij}}{\partial \mathbf{q}_{ni}^{ij}} = \frac{1}{l_r^{ij}} \mathbf{d}_{rr}^{ijT} \frac{\partial \mathbf{d}_{rr}^{ij}}{\partial \mathbf{q}_{ni}^{ij}},\\
&\frac{\partial \hat{\mathbf{d}}_{rr}^{ij}}{\partial \mathbf{q}_{ni}^{ij}} = \frac{l_r^{ij}(\partial \mathbf{d}_{rr}^{ij}/\partial \mathbf{q}_{ni}^{ij}) - \mathbf{d}_{rr}^{ij}(\partial l_r^{ij}/\partial \mathbf{q}_{ni}^{ij})}{(l_r^{ij})^2},\\
&\frac{\partial \mathbf{f}_B^i}{\partial \mathbf{q}_{ni}^{ij}} = [k_B^i \hat{\mathbf{d}}_B^i \quad \mathbf{0} \quad \mathbf{0} \quad \mathbf{0}],\\
&\frac{\partial \mathbf{f}_B^j}{\partial \mathbf{q}_{ni}^{ij}} = [\mathbf{0} \quad \mathbf{0} \quad k_B^j \hat{\mathbf{d}}_B^j \quad \mathbf{0}],\ \frac{\partial \mathbf{f}_{rr}^{ij}}{\partial \mathbf{q}_{ni}^{ij}}\\
&\qquad = k_{rr}^{ij} \left(\hat{\mathbf{d}}_{rr}^{ij} \frac{\partial l_r^{ij}}{\partial \mathbf{q}_{ni}^{ij}} + (l_r^{ij} - l_{ro}^{ij}) \frac{\partial \hat{\mathbf{d}}_{rr}^{ij}}{\partial \mathbf{q}_{ni}^{ij}} \right),\\
&\frac{\partial Q_r^i}{\partial \mathbf{q}_{ni}^{ij}} = [0 \quad -k_r^i \quad 0 \quad 0],\ \frac{\partial Q_r^j}{\partial \mathbf{q}_{ni}^{ij}} = [0 \quad 0 \quad 0 \quad -k_r^j]
\end{aligned}\right\} \tag{44}$$

In this equation, $\mathbf{u}_r^{\ k} = \mathbf{A}^k \mathbf{u}^-_{\ r}{}^k, k = i, j$. Using the definitions of (44), one can show that the 4×4 matrix associated with the coupler ij that can be used to construct the coefficient matrix in (42) is defined as

$$\frac{\partial \mathbf{Q}_{ni}^{ij}}{\partial \mathbf{q}_{ni}^{ij}} = \begin{bmatrix}
-\mathbf{L}_{Bd}^{iT} \left(\frac{\partial \mathbf{f}_B^i}{\partial \mathbf{q}_{ni}^{ij}} + \frac{\partial \mathbf{f}_{rr}^{ij}}{\partial \mathbf{q}_{ni}^{ij}} \right) \\
-\mathbf{L}_r^{iT} \frac{\partial \mathbf{f}_{rr}^{ij}}{\partial \mathbf{q}_{ni}^{ij}} - \mathbf{f}_{rr}^{ijT} \frac{\partial \mathbf{L}_r^i}{\partial \mathbf{q}_{ni}^{ij}} + \frac{\partial Q_r^i}{\partial \mathbf{q}_{ni}^{ij}} \\
-\mathbf{L}_{Bd}^{jT} \left(\frac{\partial \mathbf{f}_B^j}{\partial \mathbf{q}_{ij}^{ij}} - \frac{\partial \mathbf{f}_{rr}^{ij}}{\partial \mathbf{q}_{ni}^{ij}} \right) \\
\mathbf{L}_r^{jT} \frac{\partial \mathbf{f}_{rr}^{ij}}{\partial \mathbf{q}_{ni}^{ij}} + \mathbf{f}_{rr}^{ijT} \frac{\partial \mathbf{L}_r^j}{\partial \mathbf{q}_{ni}^{ij}} + \frac{\partial Q_r^j}{\partial \mathbf{q}_{ni}^{ij}}
\end{bmatrix} \tag{45}$$

This matrix is nonsingular in the case of nonzero stiffness coefficients k_B^i, k_B^j, and k_{rr}^{ij}. It is also important to point out, as previously mentioned in Sect. 3 that since d^i and d^j are considered as independent noninertial coordinates, these coordinates are predicted when evaluating the right-hand side of (42) and the force vector associated with the inertial coordinates using the equation $(\bar{\mathbf{u}}_d^k - ((\mathbf{R}^k - \mathbf{R}_o^k)^T \hat{\mathbf{d}}_B^k) \hat{\bar{\mathbf{d}}}_B^k - l_o^k \hat{\bar{\mathbf{d}}}_B^k)^T \hat{\bar{\mathbf{d}}}_B^k, k = i, j$.

9 Two-car model

The main goal of this study is to examine the effect of the coupler inertia on the solution accuracy and computational efficiency using simple train models. To this end, two different models are developed. The first model is developed using a general MBS algorithm that employs redundant coordinates and allows for the solution of DAE systems. This model, which accounts for the coupler inertia, is called the inertial coupler model. The second model is developed using the LTD algorithms implemented in ATTIF code. This algorithm is modified to allow for the solution of the quasistatic coupler algebraic equations with the differential equations of motion. In this second model, which is referred to as the noninertial coupler model, the effect of the coupler inertia is neglected.

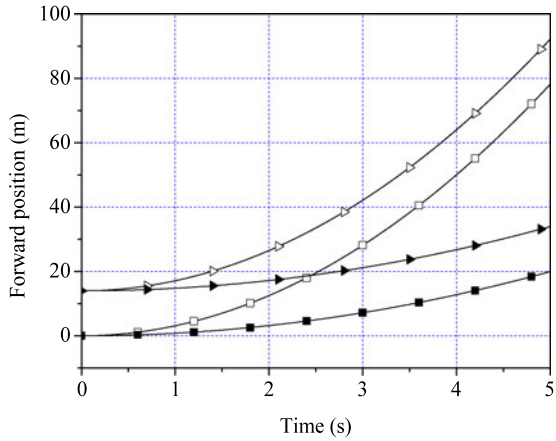

Fig. 4 Forward position (—■— Rear car loaded, —▶— Leading car loaded, —□— Rear car empty, —▷— Leading car empty)

Table 1 Model parameters

Coupler parameter	Value	Coupler parameter	Value
l_0 (m)	0.289	c_r^i, c_r^j (N·m·s)	1.0×10^5
k_B^i, k_B^j (N/m)	3×10^7	k_{rr}^{ij} (N/m)	5.0×10^8
c_B^i, c_B^j (N·s/m)	2.5×10^5	c_{rr}^{ij} (N·s/m)	5.0×10^5
k_r^i, k_r^j (N·m)	3×10^7	l_{r0} (m)	0.204

The type of coupler considered in this numerical investigation is called *long shank E-type*, which has properties reported in the literature [5]. The simple two-car train model, shown in Fig. 3, is used to obtain the numerical results reported in this numerical investigation. The coupler stiffness and damping coefficients are assumed as $k_B = k_B^i = k_B^j, c_B = c_B^i = c_B^j, k_r = k_r^i = k_r^j, c_r = c_r^i = c_r^j, k_{rr} = k_{rr}^{ij}$, and $c_{rr} = c^{ij}{}_{rr}$, with the values shown in Table 1. The masses and mass moments of inertia of the coupler components are assumed as $m_{\text{shank}} = 140$ kg, $I_{zz,\text{shank}} = 8$ k g ·m^2, and $m_{\text{EOC}} = 50$ kg. In order to examine the effect of the coupler inertia, two different simulation scenarios are considered in this investigation; the first is with empty cars, while the second is with full loaded cars.

Table 2 Car parameters

Parameter	Full loading	Empty
m (kg)	93800	23800
I_{xx} (kg·m^2)	117000	20900
I_{yy} (kg·m^2)	1370000	237000
I_{zz} (kg·m^2)	1380000	243000
I_{xy}, I_{xz}, I_{yz} (kg·m^2)	0	0

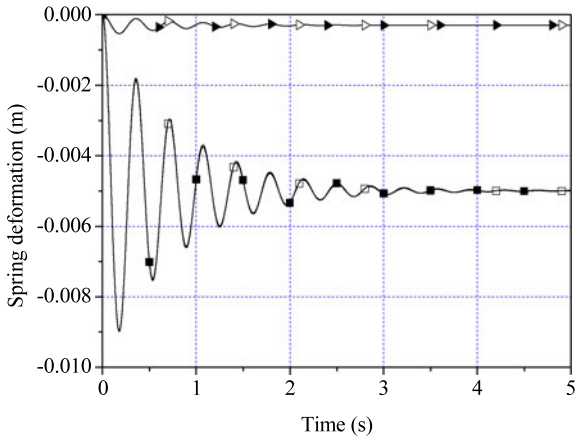

Fig. 5 EOC and shank knuckle relative displacements (loaded car scenario) (d_d^i inertial, d_d^i noninertial, d_{rr}^{ij} inertial, d_{rr}^{ij} noninertial)

In both scenarios, the traction force is applied to the rear car with a magnitude of 3×10^5 N. For both scenarios, the initial velocities and angles are assumed to be zero. The initial coordinates of the center of mass of the two cars along the longitudinal global X axis are assumed to be 0 m for the rear car and 13.976 m for the leading car; while the vertical Z coordinate of the center of mass is assumed to be 1.85 m for the full loading condition and 1.085 m for the empty condition. The inertial properties of the cars in the empty and full cases are reported in Table 2 [16]. In case of full loaded car, the ratio of the mass of the coupler to the mass of the car is 0.00205; while in the case of empty car, this ratio is 0.00798. Note that this ratio is less than 1%, even in the case of the empty car. The coupler model considered in this investigation is assumed to have EOC unit.

9.1 Simulation results

Figure 4 shows the forward position of the two cars, for the two scenarios of empty and loaded cars. Their

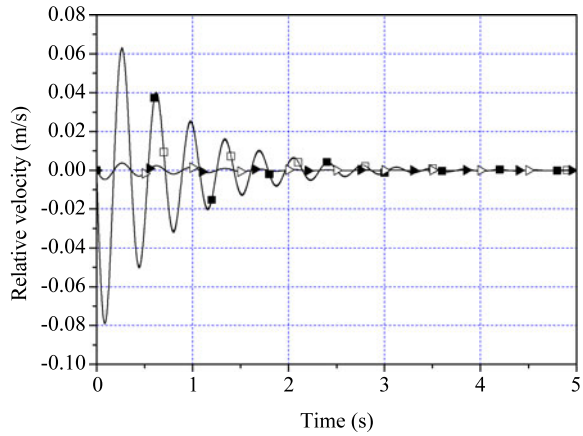

Fig. 6 EOC and shank knuckle relative velocities (loaded car scenario) ($\dot{d}_d^i$ inertial, $\dot{d}_d^i$ noninertial, $\dot{d}_{rr}^{ij}$ inertial, $\dot{d}_{rr}^{ij}$ noninertial)

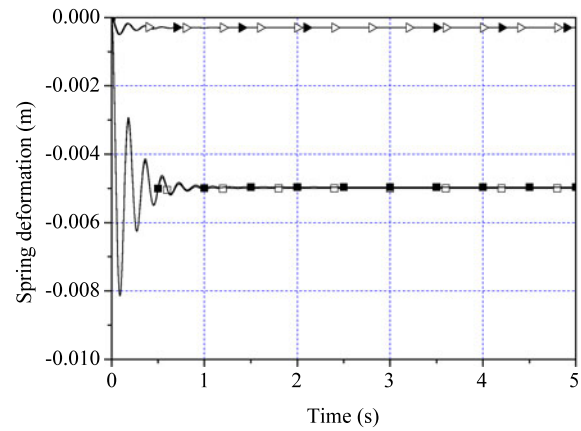

Fig. 7 EOC and shank knuckle relative displacements (empty car scenario) (d_d^i inertial, d_d^i noninertial, d_{rr}^{ij} inertial, d_{rr}^{ij} noninertial)

velocities increase linearly due to the application of the constant force. Figure 5 shows the EOC and shank knuckle relative displacements $d_d^{\,i}$ and $d^{ij}{}_{rr}$, respectively, for the full loaded car scenario using both the MBS and LTD algorithms, while Fig. 6 shows the time derivatives of these relative displacements. Figure 7 shows the EOC and shank knuckle relative displace-ments $d_d^{\,i}$ and $d^{ij}{}_{rr}$, respectively, for the empty car sce-nario using both the MBS and LTD algorithms, while Fig. 8 shows the time derivatives of these relative dis-placements. Each of these figures shows the effect of neglecting the coupler inertia.

The results presented in this section demonstrate that neglecting the coupler inertia does not have a significant effect on the accuracy of the solution. Nonetheless, the neglect of the coupler inertia leads to significant improvement in the computational efficiency. The LTD model that does not take into account the effect of the coupler inertia was found to be more than 85 times faster than the MBS model that takes into account the effect of the coupler inertia. The same explicit numerical integration method is used to obtain the results of the inertial and non-inertial coupler model.

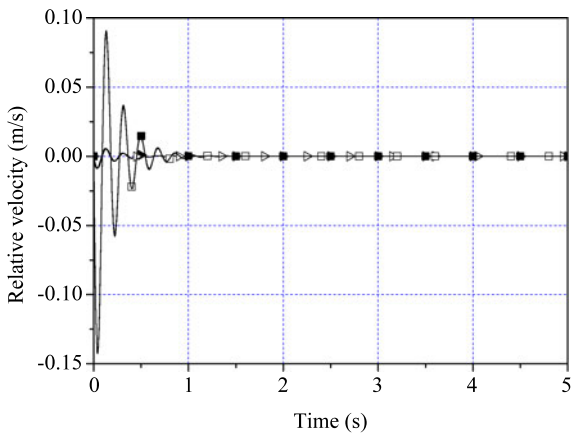

Fig. 8 EOC and shank knuckle relative velocities (empty car scenario) (—■— $\dot{d}_d^i$ inertial, —□— $\dot{d}_d^i$ noninertial, —▶— $\dot{d}_{rr}^{ij}$ inertial, —▷— $\dot{d}_{rr}^{ij}$ noninertial)

9.2 Eigen value and frequency domain analysis

Figure 9 shows the mode shapes and frequencies obtained by solving the eigenvalue problem of the inertial coupler model [7, 12], for the full loaded car model. The dashed line in this figure shows the reference configuration, while the solid line shows the displaced configuration for the given mode. Using the results presented in this figure, it is possible to recognize some frequencies that are associated with the small inertia of the coupler components, including the modes that describe the rotation of the shanks or relative displacement between the slider and the car. The first mode with a low frequency of 2.8 Hz is the only mode that is present in both the inertial and noninertial coupler models. Other modes presented in Fig. 9 are mainly due to the coupler inertia. It is clear that the second mode, for example, which has frequency of approximately 63.26 Hz corresponds to the longitudi-nal motion of the coupler with respect to the car body. This frequency can be easily calculated by using the inertia of the coupler and the stiffness coefficient k_B. It is also important to point out that the highest fre-quency is associated with the rotational motion of the shanks. The mode associated with this frequency de-pends on the coupler inertia and, therefore, this mode does not appear in the noninertial system.

In order to have a better understanding of the effect of these frequencies, a Fast Fourier Transform (FFT) of the acceleration is performed [2]. The accelerations are directly related to the coupler forces and can be used as good FFT measure. Figure 10 shows the frequency domain analysis of the acceleration of the rear

Fig. 9 Mode shapes

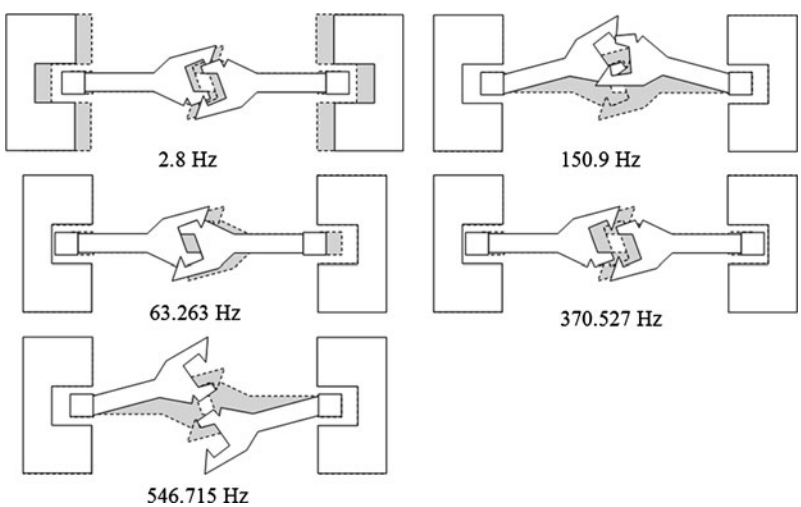

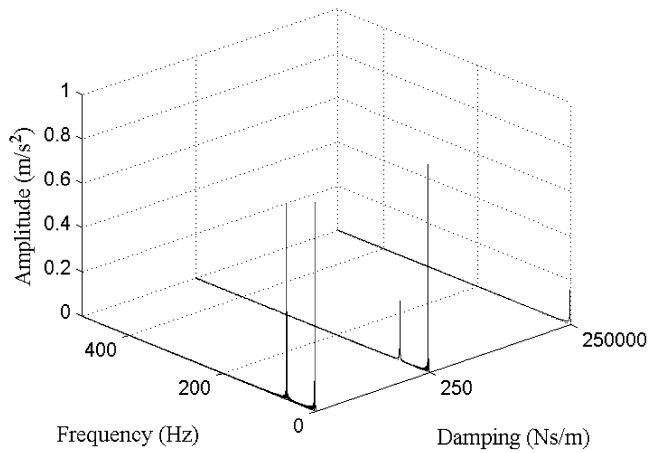

Fig. 10 Frequency domain analysis of the acceleration

coupler EOC unit which has the same frequency content as the shank acceleration. The results presented in this figure are obtained for different values of the damping coefficients c_B of the rear coupler. Figure 11 shows the frequency domain results of Lagrange multiplier associated with longitudinal generalized reaction of the revolute joint constraints of the inertial cou-pler. The results presented in this figure show clearly the effect of the first mode (2.8 Hz) and there is nearly no effect from the other higher modes.

10 Ten-car model

In order to check the robustness of the LTD coupler model implemented in ATTIF (**A**nalysis of **T**rain/**T**rack **I**nteraction **F**orces), a 10-car model is developed. This train model, shown in Fig. 12, consists of ten fully loaded cars; the cars and EOC devices have the same specifications and properties as the fully loaded cars and EOC devices used in the 2-car model discussed in the preceding section, except for the EOC damping coefficient which is assumed to be $c_B = c^i{}_B = c^j = 5 \times 10^5$ N·s/rad. The value of c_B has been chosen in order to reach steady state in a reasonable time. The tractive force is assumed to be 3×10^6 N, and the simulation is performed for 20 seconds. Figures 13 and 14 show the relative displacements and velocities of the 5th coupler using MBS and LTD algorithm. The results presented in these figures show that the LTD and MBS solutions are in a good agreement. Nonetheless, the LTD model is more than 300 times faster than the MBS model, indicating that as the number of cars increases, the LTD model will become more efficient as compared to the MBD model.

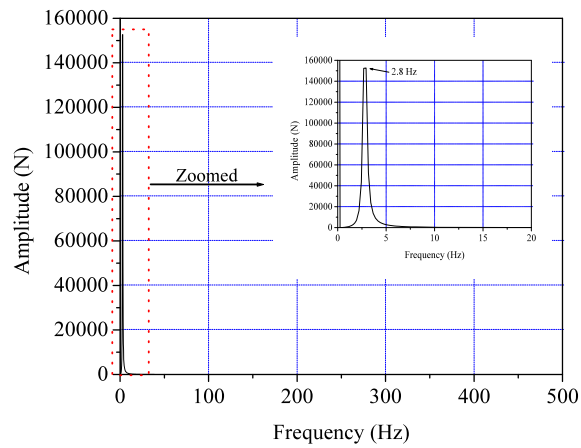

Fig. 11 Lagrange multiplier frequencies

11 Curved track simulation

In the examples considered in the preceding two sections, a tangent track was used, and therefore, α^i and α^j remain nearly constant. In order to examine the effect of the geometric nonlinearities resulting from the coupler kinematic degrees of freedom α^i and α^j; the full loaded two-car model is considered and it is assumed to negotiate the curved track shown in Fig. 15. This track is assumed to consist of 60.96 m tangent segment, 121.92 m spiral segment, 3-degree constant curve of length 91.44 m, spiral segment of length 91.44 m, tangent segment of length 121.92 m, spiral segment of length 91.44, −3-degree curve of

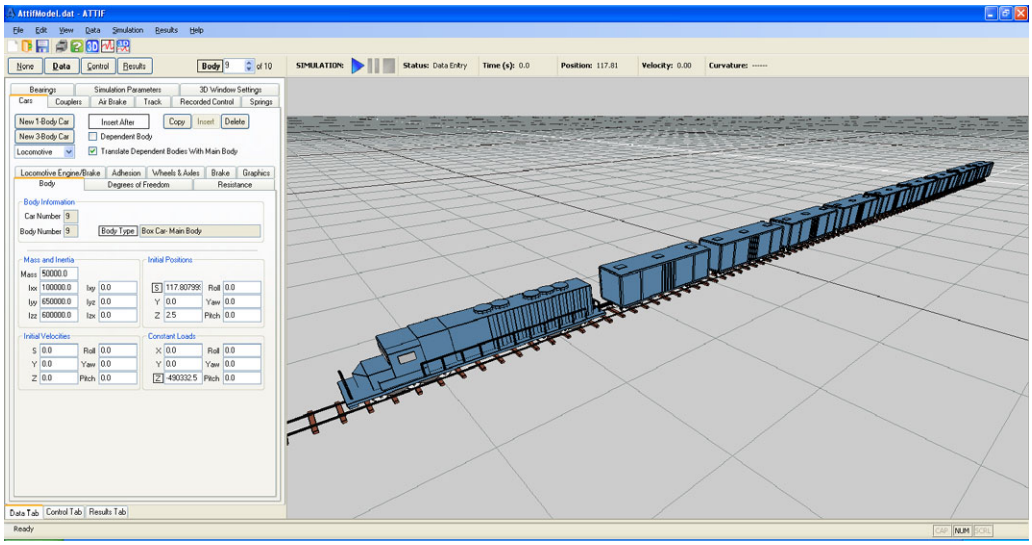

Fig. 12 Ten-car model (ATTIF interface)

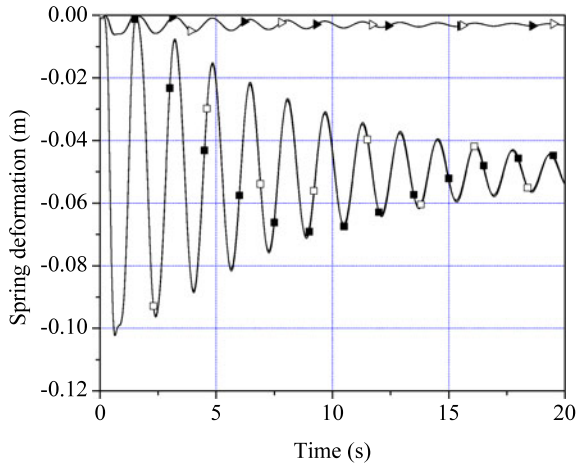

Fig. 13 EOC and shank knuckle relative displacements (5th coupler) ($\blacksquare$ d_d^i inertial, $\square$ d_d^i noninertial, $\blacktriangleright$ d_{rr}^{ij} inertial, $\triangleright$ d_{rr}^{ij} noninertial)

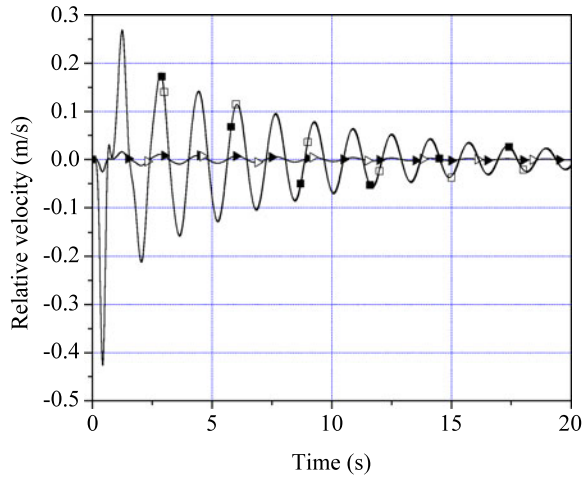

Fig. 14 EOC and shank knuckle relative velocities (5th coupler) ($\blacksquare$ $\dot{d}_d^i$ inertial, $\square$ $\dot{d}_d^i$ noninertial, $\blacktriangleright$ $\dot{d}_{rr}^{ij}$ inertial, $\triangleright$ $\dot{d}_{rr}^{ij}$ noninertial)

length of 91.44, spiral segment of length 121.92 m, and tangent segment of length 60.96. A 76.2 mm super-elevation is assumed for the first two spiral segments, and −76.2 mm for the last two spiral segments. In this example, car j is considered as the locomotive that pulls car i which represents a freight car. The length of the shank knuckle l_{r0} is assumed to be 0 m in the simulation scenario considered in this section. The initial forward velocity of each car is assumed to be 20 m/s, and the simulation time is increased to 40 s in order to capture the nonlinear behavior of the coupler on different track sections. Figure 16 shows the forward position during the first 5 seconds of car i, slider blocks i and j that represent EOC devices, and car j as the result of the application of constant forward velocity 20 m/s using both the MBS and LTD algorithms. Figure 17 shows the rotational deformation of the tor-sional spring of car i for both MBS and LTD mod-els. The results presented in these figures show that the LTD and MBS solutions are in a good agreement.

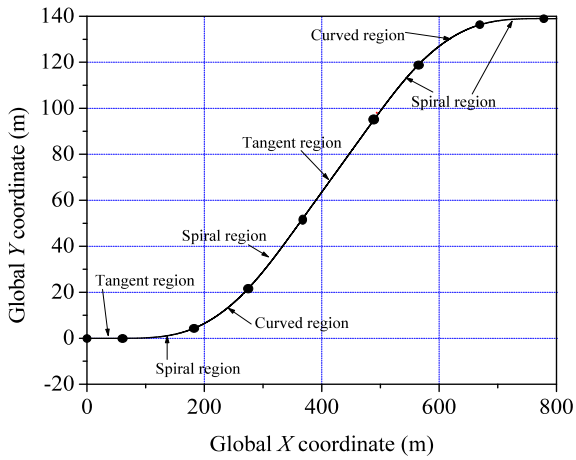

Fig. 15 Curved track

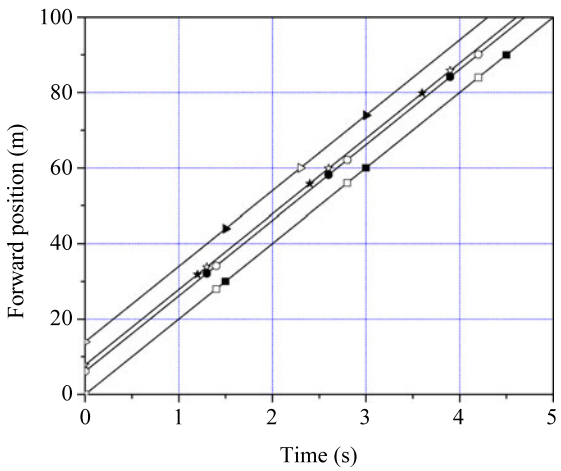

Fig. 16 Forward position (—■—Rear car inertial, —●—Slider block *i* inertial, —★—Slider block *j* inertial, —▶—Leading car inertial, —□—Rear car noninertial, —○—Slider block *i* noninertial, —☆—Slider block *j* noninertial, —▷—Leading car noninertial)

Nonetheless, the LTD model is more than 200 times faster than the MBS model, indicating that the LTD model is accurate and more efficient as compared to the MBD model in the case of curved track simulations.

12 Summary and conclusions

LTD algorithms tend to be simpler as compared to MBS algorithms that require the use of DAE solver. LTD are designed for the efficient solution and analysis of longitudinal train forces of long consists. Car coupler forces have a significant effect on the behavior of trains in response to braking, tractive, and resistance forces. For this reason, it is important to develop efficient coupler models that can be implemented in LTD algorithms. The development of such an efficient coupler model requires modifying existing LTD algorithms to include a procedure for solving differential and algebraic equations simultaneously as demonstrated in this study.

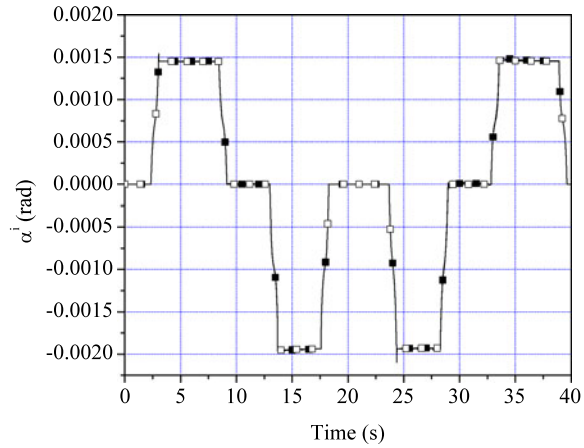

Fig. 17 Torsional spring deformation (—■—Inertial, —□—Noninertial)

This investigation is focused on studying the effect of neglecting the coupler inertia which can lead to significant deterioration of the computational efficiency. The relatively small inertia of the coupler can lead to high frequency oscillations in the solution; requiring the use of smaller integration time steps and significantly increasing the CPU time. In order to address this problem, a noninertial coupler model is developed by replacing the coupler differential equations with quasistatic nonlinear algebraic force equations. These algebraic equations are iteratively solved using a Newton–Raphson method in order to determine the noninertial coordinates. The noninertial velocities are determined by solving these quasistatic equations at the velocity level. The noninertial coordinates and velocities are then used in formulation of the generalized coupler forces associated with the coordinates of the car bodies. In order to examine the effect of neglecting the coupler inertia on the accuracy of the solution and the computational efficiency, an inertial coupler model is developed using MBS algorithms. The results obtained using the inertial and noninertial coupler mod-

els are compared. The numerical results obtained in this study showed that the neglect of the coupler inertia does not have a significant effect on the accuracy of the solution. On the other hand, the neglect of this inertia leads to significant improvement in the computational efficiency. The results obtained showed that the LTD implementation that neglects the effect of the coupler inertia becomes more efficient as the number of cars increases. An eigenvalue analysis and FFT are used to identify the frequencies associated with the coupler inertia. As discussed in this study, these high frequencies do not appear when the noninertial coupler model is used.

Acknowledgements This research was supported by the Federal Railroad Administration, Washington, DC.

References

1. Arnold, M., Burgermeister, B., Weber, S.: Improved time integration of multibody system models. In: The 1st Joint International Conference on Multibody System Dynamics, Lappeenranta, Finland (2010)
2. Brigham, E.O.: The Fast Fourier Transform. Prentice-Hall, Englewood Cliffs (1974)
3. Burgermeister, B., Arnold, M., Eichberger, A.: A quasi-static approach for constrained systems in real-time simulation. In Proc. Appl. Math. Mech., p. 7. Wiley-VCH, Weinheim (2007)
4. Cole, C., Sun, Y.Q.: Simulated comparisons of wagon coupler systems in heavy haul trains. Proc. IMechE, F, J. Rail Rapid Transit, **220**, 247–256 (2006)
5. Dawson, R.W.: The Car and Locomotive Cyclopedia, 6th edn., Sect. 6, pp. 639–703. Simmons Boardman, Omaha (1997)
6. Durali, M., Shadmehri, B.: Nonlinear analysis of train derailment in severe braking. J. Dyn. Syst. Meas. Control **125**, 48–53 (2003)
7. Genta, G.: Vibration Dynamics and Control. Springer, New York (2009)
8. Janney, E.: Improvement in car couplings, US Patent 138,405, 29 April, 1873
9. Roberson, R.E., Schwertassek, R.: Dynamics of Multibody Systems. Springer, Berlin (1988)
10. Roberts, N.L.: Coupler. US Patent 4,245,747, 20 January, 1981
11. Sanborn, G.G., Heineman, J.R., Shabana, A.A.: A low computational cost nonlinear formulation for multibody railroad vehicle systems. In: Proceedings of the ASME International Design Engineering Technical Conferences & Computer and Information in Engineering Conference, Las Vegas, NV, September 4–7, 2007
12. Shabana, A.A.: Vibration of Discrete and Continuous Systems. Springer, New York (1997)
13. Shabana, A.A.: Computational Dynamics, 3rd edn. Wiley, New York (2010)
14. Shabana, A.A., Sany, J.R.: An augmented formulation for mechanical system with non-generalized coordinates: application to rigid body contact problems. Nonlinear Dyn. **24**, 183–204 (2001)
15. Shabana, A.A., Zaazaa, K.E., Sugiyama, H.: Railroad Vehicle Dynamics: A Computational Approach. Francis & Taylor/RC, Boca Raton (2008)
16. Shabana, A.A., Aboubakr, A.K., Ding, L.: Development of a new train coupler model using non-inertial coordinates. Technical Report #MBS2010-6-UIC, Department of Mechanical Engineering, University of Illinois at Chicago, Chicago (2010)
17. Snell, F.: Railway coupler shank. US Patent 3,860,121, 14 January, 1945
18. Stronati, L.: A coupler model for the analysis of longitudinal train forces. M.Sc. Thesis, Department of Mechanical Engineering, University of Illinois at Chicago, Chicago (2010)